Energy and Buildings 55 (2012) 738–746

Contents lists available at SciVerse ScienceDirect

Energy and Buildings

journal homepage: www.elsevier.com/locate/enbuild

Experimental and numerical study of influence of air ceiling diffusers on room air flow characteristics

Mohammed A. Aziz, Ibrahim A.M. Gad, El Shahat F.A. Mohammed, Ramy H. Mohammed *

Department of Mechanical Power Engineering, Zagazig University, 44159, Egypt

ARTICLE INFO

Article history:
Received 15 September 2012
Accepted 21 September 2012

Keywords:
Ceiling diffusers
Thermal comfort
Turbulence model
Validation
Energy consumption

ABSTRACT

This paper investigates experimentally and numerically airflow characteristics of vortex, round, and square ceiling diffuser and its effect on the thermal comfort in a ventilated room. Three different thermal comfort criteria namely; mean age of the air, ventilation effectiveness, and effective draft temperature have been used to predict the thermal comfort zone inside the room. Experimentally, a sub-scale room is set-up to measure the temperature field in the room. Numerically, unstructured grids have been used to discretize the numerical domain. Conservation equations are solved using FLUENT commercial flow solver. The code is validated by comparing the numerical results obtained from three different turbulence models with the available experimental data. The validation shows that the standard k–ε turbulence model can be used to simulate these cases successfully. After validation of the code, effect of supply air velocity on the flow and thermal field is investigated and hence the thermal comfort and energy consumption. The results show that the saved energy by vortex diffuser is 1.5 times lower than that achieved by square or round diffuser. The velocity decay coefficient is nearly same for square and round diffusers and is 2.6 times greater than that for the vortex diffuser.

1. Introduction

Nowadays, the majority of people spend up to 90% of their time indoors. Knowledge and prediction of indoor climate conditions are important for optimizing indoor climate and thermal comfort, and it is also important for energy conservation [1–3]. Indoor air quality and thermal comfort are two important aspects of indoor environmental quality that receive considerable attention.

Design conditions of HVAC as specified by ASHRAE [4] are temperature, and relative humidity should be held in the range of (20–24 °C), and 50–60%, respectively. Alongside, positive air pressure should be maintained, and all air exhausted with no recirculation is preferred [5].

The mean age of air (MAA) is one of the most important parameters describing the ventilation efficiency in a space. It is defined as the average time for air to travel from a supply outlet area to any location in a ventilated room [6–8]. Its concept is assumed to be equal zero (100% fresh) at inlet. It is obvious that the high values of MAA mean that part of the air circulates for a long time inside the room. So, the values of the MAA reflect the efficiency of ventilation system.

Spitler [9] studied the effect of the inlet velocity on air distribution in a full scale unoccupied ventilated room has dimensions of 5 m long, 3 m wide, and 3 m high. The supply and exhaust outlets are each 0.333 m wide and 1.0 m high. Nielsen [10] described experiments with wall-mounted air terminal devices. This study gave expressions for the velocity distribution close to the floor. The velocity at the floor was influenced by the flow rate to the room, the temperature difference and the type of the diffuser.

Al-Hamed [2] employed a computer program for simulating 3D room ventilation problems to predict the mean air temperatures and air velocities for a number of realistic supply air inlet and outlet locations. The k–ε turbulence model was considered. The flow field predicted by this model was validated by experimental measurements done by other investigator. His study showed that the PMV occupancy comfort response was more favorable.

Srebric and Chen [11] used a simplified method to describe flow and thermal information from eight various diffusers which were nozzle diffuser, slot (linear) diffuser, valve diffuser, displacement diffuser, round ceiling diffuser, square ceiling diffuser, vortex diffuser, and grille diffuser. The box method was suitable for most of the diffusers with an appropriate box size. The momentum method was applied well for five diffusers. Since the momentum method was simpler than the box method, the momentum method should be used, whenever it is applicable.

Zhou and Haghighat [12] developed a simplified method to define the boundary conditions at the inlet of the swirl diffuser.

* Corresponding author. Tel.: +20 111 404 9331.
E-mail address: rhamdy@zu.edu.eg (R.H. Mohammed).

0378-7788/$ – see front matter © 2012 Elsevier B.V. All rights reserved.
http://dx.doi.org/10.1016/j.enbuild.2012.09.027

Nomenclature

A	inlet area [m^2]
C	concentration [m^3 of vapor/m^3 of moisture air]
C_d	discharge coefficient
C_p	pressure coefficient
d	neck diameter of diffuser [m]
E	ventilation effectiveness
g	gravity acceleration [m/s^2]
k	turbulent kinetic energy [m^2/s^2]
K	velocity decay coefficient
P	pressure [Pa]
Re	Reynolds number
RH	relative humidity [%]
Sc_{eff}	effective Schmidt number
t, T	temperature [°C, K]
t_o	temperature of a reference point [°C]
V	velocity [m/s]
x	distance [m]
x, y, z	co-ordinate system
y	vertical location [m]

Greek symbols

β	thermal expansion coefficient [1/°C]
Γ	diffusion coefficient
ε	turbulent dissipation rate [m^2/s^3]
θ	swirling angle [°]
λ	thermal conductivity [W/m °C]
μ	dynamic viscosity [Pa s]
ρ	air density [kg/m^3]
ϕ	diameter [m]

Abbreviations

3D	three dimensions
CFD	computational fluid dynamics
EDT	effective draft temperature
HVAC	heating, ventilation and air conditioning
LDA	laser Doppler anemometry
MAA	mean age of the air
PIV	particle image velocimetry
PMV	predicted mean vote
PTV	particle tracking velocimetry
RNG	re-normalization group
T.C	thermocouple

Subscripts

d	digital manometer
e	exit
m	mean
o	inlet conditions
s	supply

With this method a round diffuser was divided into six triangular sectors with equal air discharge rate, while various air throw orientation angles were assigned to each sector. Comparisons between smoke airflow visualization and CFD predictions demonstrated the effectiveness of the current simplified modeling method of swirl diffuser. Profiles of temperature and air velocity from measurements were also presented to validate the CFD simulation results. This validation showed that the simplified method can be used to model the diffusers.

Einberga and Hagstrom [13] discussed the modeling results from CFD simulation of a multi-cone air diffuser for industrial spaces. CFD simulations were compared systematically with data from experimental measurements while air velocity was measured by ultrasonic sensors. The outcomes of this study showed that CFD simulation with a standard k–ε model accurately predicted non-isothermal airflow around the diffuser.

The majority of previous studies in indoor airflows were conducted in reduced scale rooms and the numerical simulations were compared to the reduced scale experiments. There was a lack of experimental data available to validate mathematical models. The previous studies were not agreed on the suitable turbulence model that more valid. Also, there was not a clear vision about the diffusers energy consumption. As a result, some fundamental issues remain unsolved related to the predictability of existing mathematical models for low Reynolds number flows.

The important goal of this study is to improve the analysis of real life environments. Thus, particular emphasis is placed on the complexity of the diffuser geometry where the three-dimensional (3D) flow occurs. Evaluation of the performance of three ceiling diffusers is performed and the more suitable turbulence model for these cases is specified. Also, the region of the thermal comfort is predicted. The diffusers energy consumption is determined. This investigation of the air diffusers characteristics and its impact on the indoor airflows is conducted through two approaches: experimental measurements and numerical simulations.

2. Experimental work

2.1. Experimental set-up

The general layout of the experimental set-up is shown in Fig. 1. It is consists of two main parts namely: air conditioning unit and test rig (model room).

The air conditioning unit is a simple vapor compression refrigeration cycle which used to deliver cold air to the test room. A fan pulls atmospheric air and passing it over evaporator. Cubic glassed model room is fabricated from Perspex has 1 m long. The round supply duct has 15 cm diameter that runs from the air conditioning to the inlet of the test room.

The supply duct is fitted with discharge control gate in the form of the vortex diffuser which vanes can turn for changing the air volume flow rate supplied to the room. The airflow enters the room from an opening at its ceiling of 15 cm diameter in which tested diffuser is installed.

The temperatures of floor, ceiling of the room, and air are measured by means of copper-constantan thermocouples (T-type). A sliding arm having fixed thermocouple at its terminal end is installed at the corner of the room, it can move along three dimensions to measure the temperature inside the room (Fig. 1). Thermocouple is fixed just before the outlet diffuser to measure the inlet temperature. Alongside, other thermocouples are mounted on the four walls, floor, and the roof. All thermocouples are connected to switches followed by digital thermometer. The thermocouples readings are measured from digital thermometer which has uncertainty of ±0.2 °C of received readings according to its manual data.

Digital manometer is used to measure the air velocity (V_d) before the diffuser and hence, the air flow rate can be measured. The error of the measured value is about ±0.1 m/s. The pressures drop a cross orifice meter is measured by using inclined water manometer having error about ±0.1 mm H_2O. The calibrations of the instruments should be carried out in this type of tests. T-type thermocouples are calibrated by a direct comparison method, where the readings of the thermocouples are compared with those of standard mercury-in-glass thermometers. The calibration process has been performed in temperature variation range of 14–97 °C for heating mode, and 95–17 °C for cooling mode. Also, other instruments are calibrated by using this methodology.

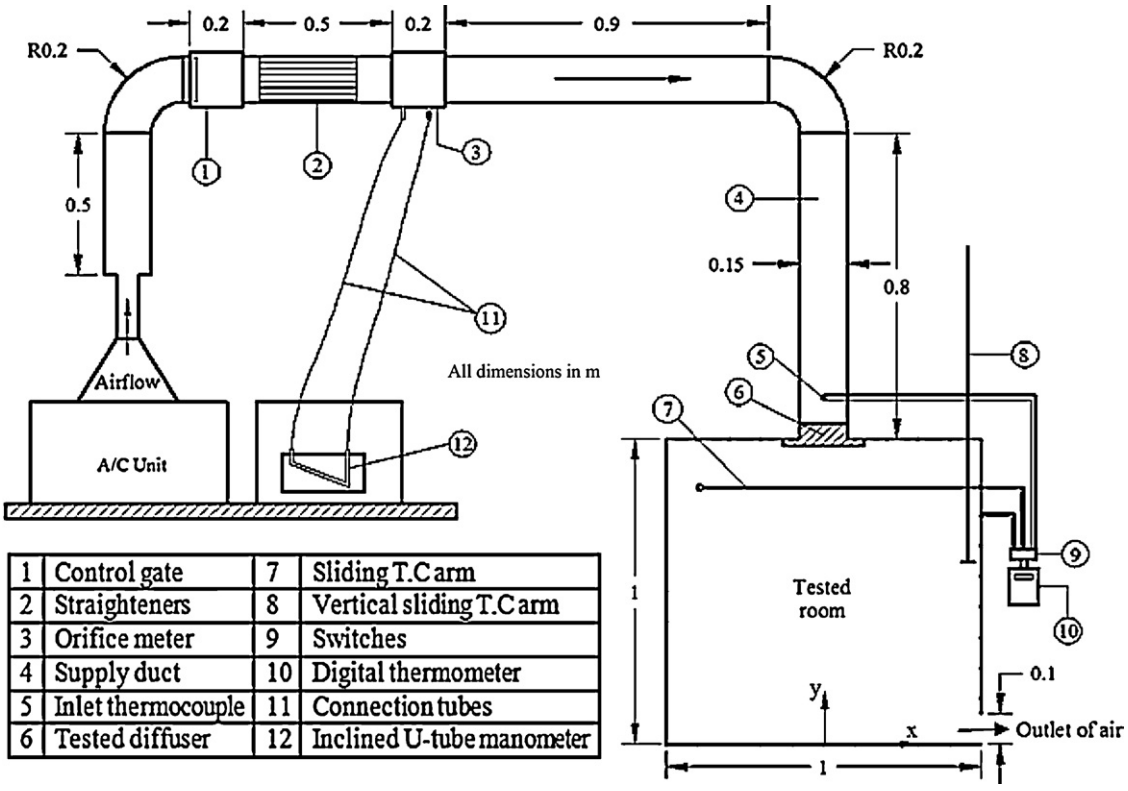

Fig. 1. Schematic diagram of the experimental set-up.

2.2. Uncertainty estimation

The compound variables such as air density, discharge flow coefficient, and ventilation effectiveness can be calculated as follows and summarized in Table 1:

- The uncertainty associated with air density (U_ρ) can be written as:

$$U_\rho = \frac{\partial_\rho}{\partial T} U_T \tag{1}$$

- The uncertainty associated with discharge flow coefficient (U_{Cd}) can be written as:

$$U_{C_d}^2 = \left[\left(\frac{\partial C_d}{\partial V_d} U_{V_d} \right)^2 + \left(\frac{\partial C_d}{\partial \rho} U_\rho \right)^2 + \left(\frac{\partial C_d}{\partial \Delta H} U_{\Delta H} \right)^2 \right] \tag{2}$$

- The uncertainty associated with ventilation effectiveness (U_E) can be written as:

$$U_E^2 = \left[\left(\frac{\partial E}{\partial t_s} U_{t_s} \right)^2 + \left(\frac{\partial E}{\partial t_m} U_{t_m} \right)^2 + \left(\frac{\partial E}{\partial t_e} U_{t_e} \right)^2 \right] \tag{3}$$

Table 1
Uncertainty of compound variable.

Compound variable	Uncertainty
Air density	0.066%
Discharge flow coefficient	2.245%
Ventilation effectiveness	6.88%

2.3. Experimental procedure

In the present work, mainly three types of ceiling diffusers are involved. These diffusers are namely; vortex (swirl), round, and square ceiling diffusers. Geometry of these diffusers is shown in Fig. 2. Each diffuser is installed and investigated sequentially. The range of the studied inlet air velocity is from 1 to 4 m/s.

Zero readings of all instruments should be settled. The air conditioning unit is switched on and air flow rate is then adjusted by means of the vortex control gate. On achieving the steady state conditions, a number of temperatures are carried out subsequently averaged. The number of successive measurements depends on the degree of steadiness of the temperature. The system is allowed time to stabilized after each adjustment. It is considered steady state when temperatures agreed within 2% between two consecutive readings taken every 3 min. The steady state has been observed about 15 min. After achieving the steady state, the pressure drop across orifice meter, the room air inlet temperature, and T-type thermocouple readings inside the room are recorded. These procedures are then repeated through succession value of the input flow rate of the supply air.

3. Numerical model

The numerical study is conducted to simulate the airflow in a sub-scale room. The steady, viscous, 3D governing equations, and the mean age of air transport equation representing the flow field are solved. The FLUENT package includes FLUENT 6.3.26 [14] and GAMBIT 2.4.6 are used to simulate the problem under this consideration. Indoor airflow calculations use the Boussinesq approximation for thermal buoyancy [15]. This approximation takes air density as constant in the momentum terms and considers the buoyancy influence on air movement by the difference between the local air weight and the pressure gradient. With an

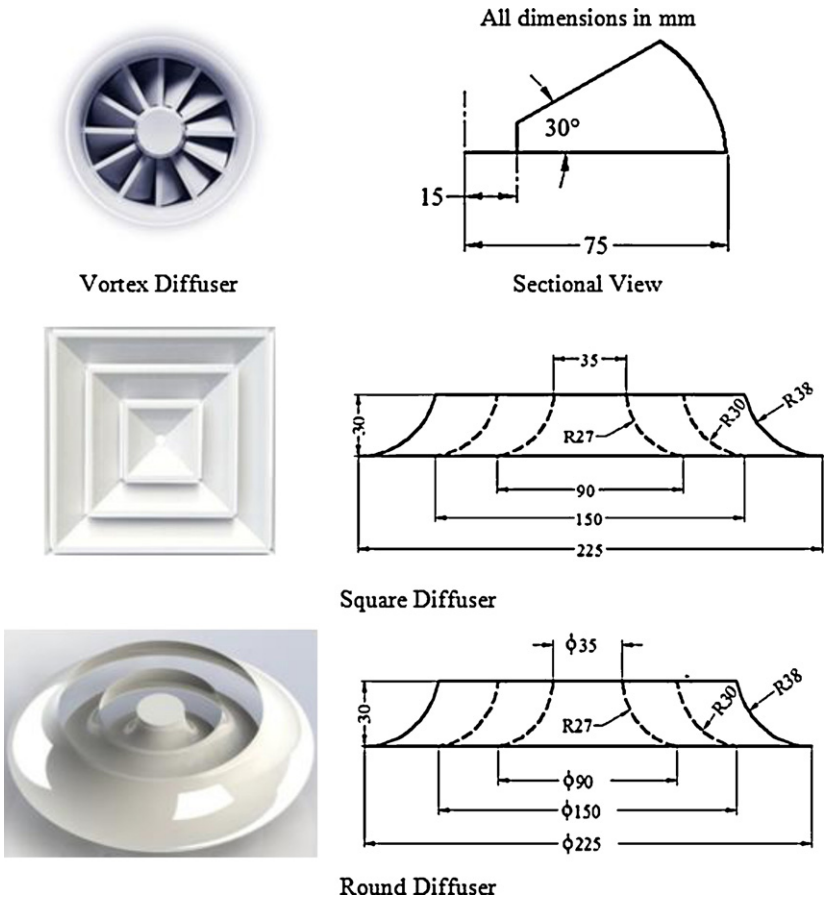

Fig. 2. Simulated diffusers geometry.

eddy-viscosity model, the indoor airflow is described by the following time-averaged Navier–Stokes equations for the conservation of mass, momentum, energy, and species transport equation [16–18].

• Continuity equation

$$\nabla \cdot V = 0.0 \tag{4}$$

• Momentum equation

$$\rho V.\nabla V = -\nabla P + \mu_{eff}\nabla^2 V + \rho g\beta(T - T_{ref}) \tag{5}$$

where ρ = air density, V = velocity, P = pressure, μ_{eff} = effective dynamic viscosity, β = thermal expansion coefficient of air, T_{ref} = temperature of a reference point, t = temperature; g = gravity acceleration. The last term on the right side of Eq. (2) is the buoyancy term. The turbulent influences are lumped into the effective viscosity as the sum of the turbulent viscosity μ_t and laminar viscosity μ_l:

$$\mu_{eff} = \mu_t + \mu_l \tag{6}$$

• Energy equation

The energy equation describes the temperature distribution throughout the non-isothermal flow domain. This equation is derived from the first law of thermodynamics to the elemental central volume as following:

$$\rho C_P V \cdot \nabla T = \lambda_{eff}\nabla^2 T \tag{7}$$

where C_p is the specific heat at constant pressure (J/kg °C) and λ_{eff} is the effective thermal conductivity (W/m °C) which can be expressed as,

$$\lambda_{eff} = \lambda_l + \lambda_t \tag{8}$$

where λ_l is the laminar thermal conductivity and λ_t is the turbulent thermal conductivity which depends on the local flow field.

• Concentration of species equation

$$\frac{\partial_\rho V_j C}{\partial x_j} = \frac{\partial}{\partial x_j}\left[\Gamma_{c,eff}\left(\frac{\partial C}{\partial x_j}\right)\right] + S_C \tag{9}$$

where C is species concentration; $\Gamma_{c,eff}$ is effective turbulent diffusion coefficient for C; S_C is source term of C. Similar method to the energy equation is used to determine the effective diffusive coefficient for species concentration $\Gamma_{c,eff} = \mu_{eff}/Sc_{eff}$ where effective Schmidt number, Sc_{eff}, is equal to 1.0.

• Standard k–ε model

$$\frac{\partial}{\partial x_i}(\rho u_i k) = \left(\mu + \frac{\mu_t}{\sigma_k}\right)\nabla^2 k + \mu_t S^2 - \rho\varepsilon \tag{10}$$

$$\frac{\partial}{\partial x_i}(\rho u_i \varepsilon) = \left(\mu + \frac{\mu_t}{\sigma_\varepsilon}\right)\nabla^2 \varepsilon + C_{\varepsilon 1}\frac{\varepsilon}{k}\mu_t S^2 - C_{\varepsilon 2}\rho\frac{s^2}{k} \tag{11}$$

$$\mu_t = \frac{\rho C_\mu k^2}{\varepsilon} \tag{12}$$

The coefficients are (C_μ, σ_k, σ_ε, $C_{\varepsilon 1}$, $C_{\varepsilon 2}$) = (0.09, 1.0, 1.3, 1.44, 1.44) and $S = (S_{ij}S_{ij})^{0.5}$.

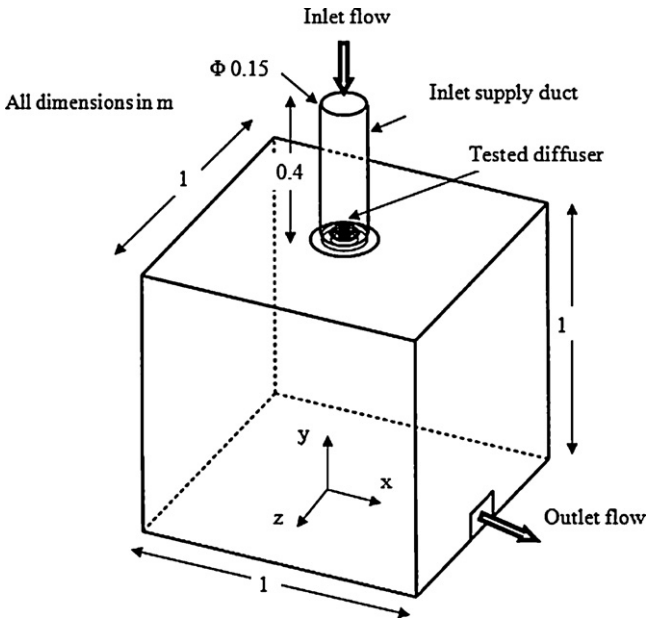

Fig. 3. Computational domain.

The thermal comfort indices which used in this study can be calculated as following:

• Mean age of the air (MAA)

The mean age of air can be calculated according to ASHRAE standard from the following transport equation:

$$\frac{\partial}{\partial x_i}\left(\rho u_i \mathrm{MAA} - \left(2.88\rho \times 10^{-5} + \frac{\mu_{eff}}{0.7}\right)\frac{\partial \mathrm{MAA}}{\partial x_i}\right) = S \quad (13)$$

where S is the source term, which depends on the density of the air mixture [6,7].

The MAA is not directly available from Fluent so, it is programmed and calculated as user-defined scalars.

• Overall ventilation effectiveness (E)

The overall ventilation effectiveness represents the effectiveness of energy utilization supplied into the occupied zone to achieve a satisfactory thermal comfort level [8].

$$E = \frac{t_e - t_s}{t_m - t_s} \times 100 \quad (14)$$

• Effective draft temperature (EDT)

The EDT index is combination of temperature and air velocity. The values of the effective draft temperature between −1.7 and 1.1 characterize the thermal comfort [1]. Values less than −1.7 represent cool sensation while values above 1.1 represent warm sensation. This expression for EDT is given by:

$$\mathrm{EDT} = (t_x - t_m) - 8(V_X - 0.15) \quad (15)$$

Fig. 3 shows the computational domain which consists of four walls, ceiling, and floor. Each has 1 m height and 1 m width and outlet opening is of 0.17 m width and 0.1 m height. Vortex, square, and round diffusers (manufactured by TROX) are simulated. Each diffuser has 15 cm neck diameter. It is conducted into the computational domain to study its effect on the airflow characteristics.

Table 2
Boundary conditions.

Boundary	Velocity	Temperature	Relative humidity
Supply	$-V_y = 1$–4 m/s $V_x = V_z = 0.0$	18 °C	60%
Exhaust	(V_x, V_y, V_z)[a]	(t)[a]	(RH)[a]
Walls	$V_x = V_z = V_x = 0.0$	$t = 28.5$	0
Ceiling	$V_x = V_z = V_x = 0.0$	$t = 27$	0
Floor	$V_x = V_z = V_x = 0.0$	Adiabatic ($q = 0$)	0
Diffuser	$V_x = V_z = V_x = 0.0$	Adiabatic ($q = 0$)	0
Inlet duct	$V_x = V_z = V_x = 0.0$	Adiabatic ($q = 0$)	0

[a] Unknown, to be solved as a part of numerical solution.

3.1. Boundary conditions

No-slip boundary conditions are used along the room walls, the ceiling, and the floor. All walls and ceiling are isothermal with specified temperature that will be mentioned in the simulation. The floor and the inlet duct are assumed to be adiabatic walls which the temperature gradient or heat transfer flux is zero. The diffuser vanes (blades) have been included in the calculation domain as a solid surface with zero heat flux.

Values of the boundary conditions are evaluated through experimental measurements. All properties are assumed to be uniform across the inlet section. The properties specified include velocity in one dimension, relative humidity, and temperature. Furthermore, for turbulent flows, turbulence intensity and hydraulic diameter are set at the inlet section. For all cases, 8% turbulence intensity and 0.15 m hydraulic diameter are used. At the outflow boundary, environmental pressure is considered where the boundary values are estimated by extrapolation from the interior points. The present CFD code required initial conditions throughout the domain to start the solution. Numerical values of the boundary conditions used for the solution are listed in Table 2. The constant fluid properties are taken at a reference temperature of $T_{ref} = 20\,^{\circ}\mathrm{C} = 293.15$ K as follows:

$\mu = 1.8 \times 10^{-5}$ kg/(m s), $C_p = 1004$ J/(kg K), $k = 0.026$ W/(m K), $\rho = 1.2$ kg/m^3, $\beta = 0.0034$ K^{-1}.

3.2. Mesh sensitivity

Several unstructured grids are performed with different mesh sizes for each diffuser to guarantee the grid independence of the results. Fig. 4 shows the temperature and velocity distribution

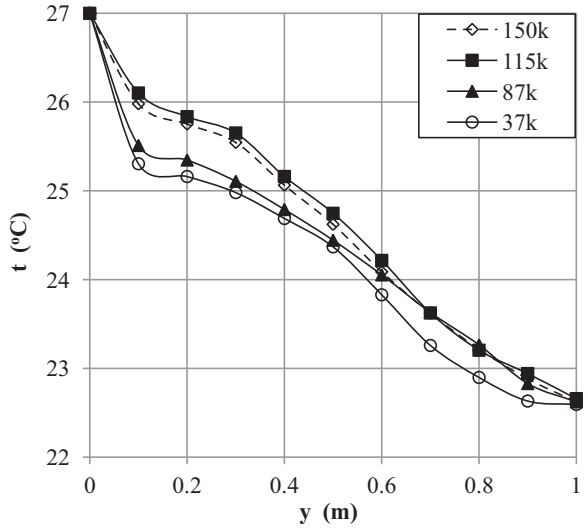

Fig. 4. Temperature distribution over vertical line at the center of the room for different grid sizes – vortex diffuser.

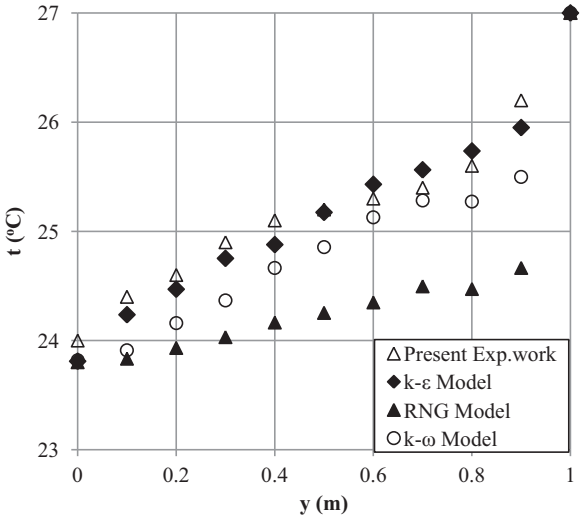

Fig. 5. Temperature distribution measured by present work and predicted by three types of turbulence models – vortex diffuser.

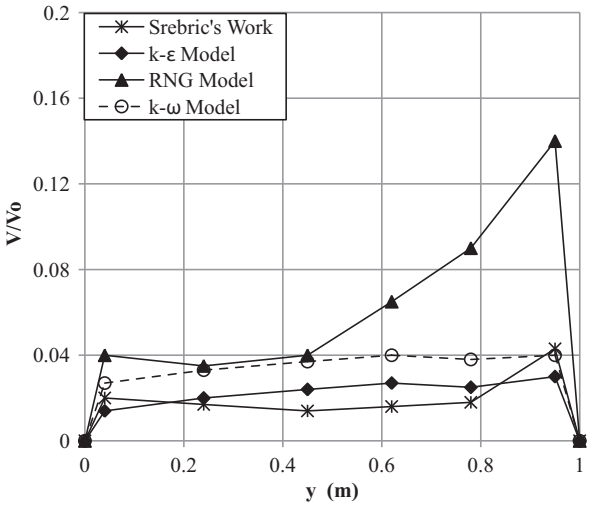

Fig. 6. Comparison between (V/V_o) distributions measured by Srebric and Chen [11] and predicted by three types of turbulence models – vortex diffuser.

respectively over vertical line at the center of the room for 37,000 (37k), 87,000 (87k), 115,000 (115k), and 150,000 (150k) grid sizes. According to this figure, the obtained results with 115k and 150k are very close where the maximum percentage error is about 0.4%. Therefore, the results from 150k grid size can be considered to be grid independence.

4. Code validation

One case of the vortex diffuser with 45° swirling angle is selected to establish the validation process where the three different types of the turbulence models namely; standard k–ε, RNG k–ε, and standard k–ω are investigated. A comparison between the predicted results obtained from these turbulence models, the present available experimental data, and the previous measurements by Srebric and Chen [11] is performed.

Fig. 5 shows comparison between the predicted temperature distributions and the present measured temperatures over the vertical line. Fig. 6 shows comparison between the vertical dimensionless velocity distributions (V/V_o) obtained from the three considered turbulence models and Srebric's measurements. Also, both square and round diffusers are validate and create the same trend and behavior. Accordingly, the standard k–ε turbulence model can be used to simulate indoor airflow with good agreement and accuracy of 0.77%.

5. Results and discussion

5.1. Description of air flow emerged from the ceiling diffusers

Fig. 7a presents the path lines exit from the vortex diffuser with 45° swirling angle. The swirling jet flow from this diffuser reaches to the middle of the room. The throw of the diffuser seems as a short and the swirl flow diminishes at the middle height of the room therefore, there is no vortex or swirl flow on the lower half of the room (occupied zone). In the same way, the flow of the round diffuser emerges radically and reaches to the side walls then it turns 90° downward and a vortex ring is create near the ceiling. The throw of the round diffuser is noticeably longer as shown in Fig. 7b. The velocity vectors from the square diffuser are shown in Fig. 7c. The throw of this diffuser seems a long where the flow just reaches to the side walls. After the flow reaches to the walls, it turns 90° downward, where two vortexes create next to the vertical walls and the ceiling in the upper corner of the room. This figure shows that the emerged air jet from the square diffuser has two dimensions without any swirling flow.

5.2. Effect of the inlet velocity

Fig. 8 shows the relationship between the pressure coefficient and Reynolds number for the three diffusers. Both pressure coefficient and Reynolds number can be calculated from Eqs. (16) and

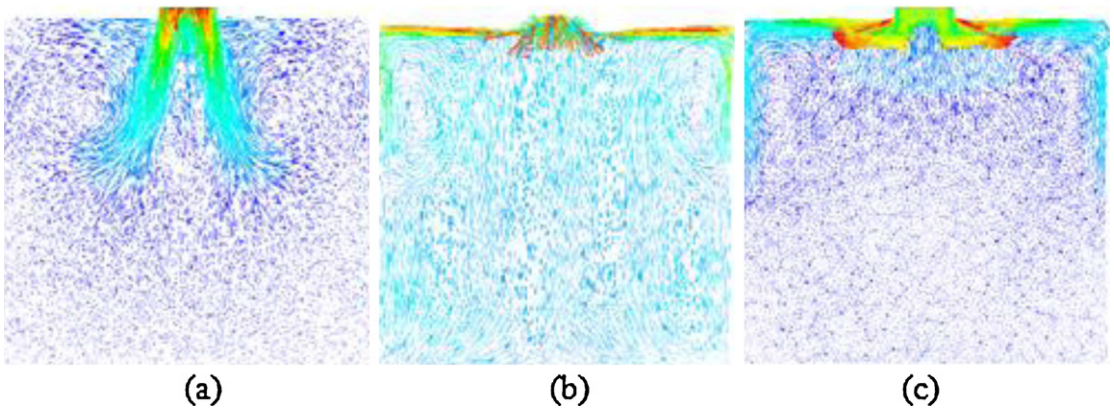

Fig. 7. Velocity vector at the vertical plane for (a) vortex, (b) round, and (c) square diffuser at V_o = 1 m/s and t_o = 18 °C.

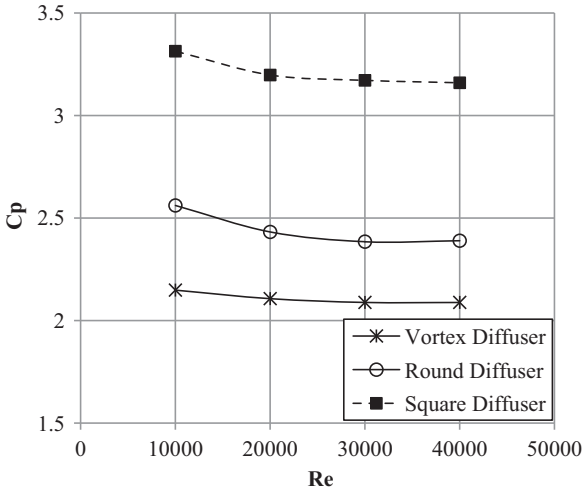

Fig. 8. Pressure coefficient at different Reynolds number for different diffusers.

(17), respectively. The pressure coefficient considers a pointer on the energy consumption.

$$C_p = \frac{\Delta p}{1/2\rho V^2} \tag{16}$$

$$Re = \frac{\rho V d}{\mu} \tag{17}$$

From Fig. 8, it is clear that all three tested diffusers have the same trend. The highest values of C_p belong to the square diffuser while the minimum values belong to the vortex one.

The dimensionless mean velocity (V_m/V_o) is plotted with Reynolds number (Re) as in Fig. 9. From this figure, it is clear that the dimensionless mean velocity V_m/V_o increases with Reynolds number in case of the round diffuser only.

Fig. 10 shows the effect of the Reynolds number on the dimensionless mean temperature. The room seems as cool in case of the vortex diffuser because the cold air jet from the vortex diffuser is focused and concentrated on the middle of the room.

Fig. 11 shows the relation between the dimensionless mean relative humidity in the room and Reynolds number. As the air inlet velocity increases by 1 m/s, the mean value of the relative humidity

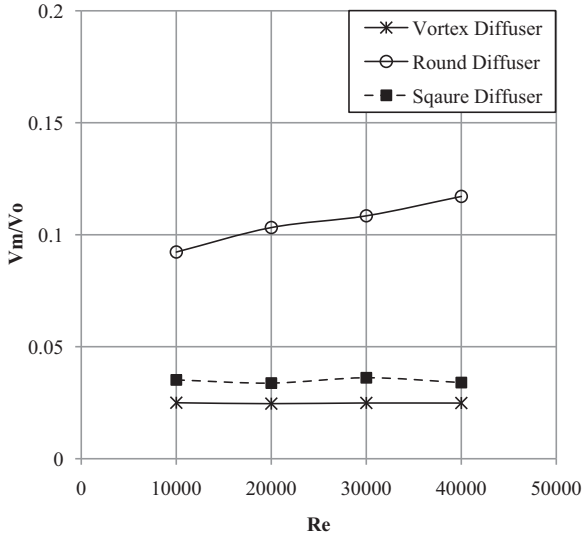

Fig. 9. Dimensionless mean velocity at different Reynolds numbers for different diffusers at same inlet temperature and relative humidity.

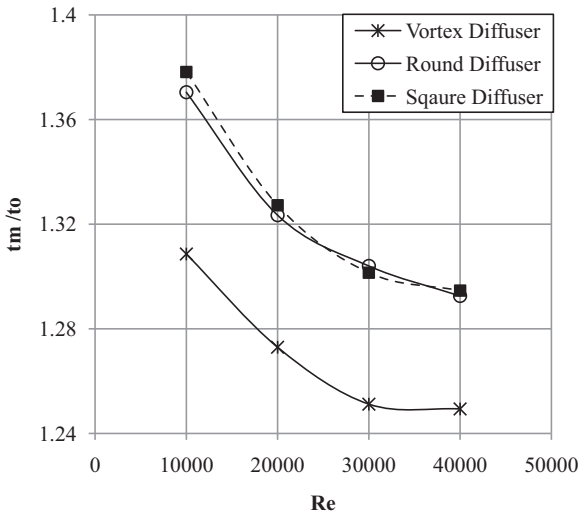

Fig. 10. Dimensionless mean room temperature at different Reynolds numbers for different diffusers at same inlet temperature and relative humidity.

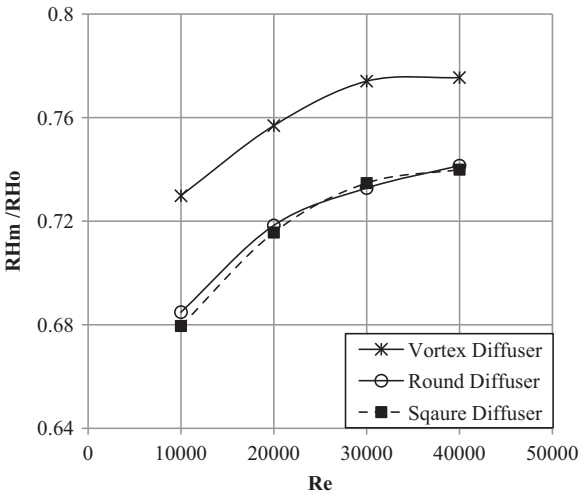

Fig. 11. Dimensionless mean room relative humidity at different Reynolds numbers at same inlet temperature and relative humidity.

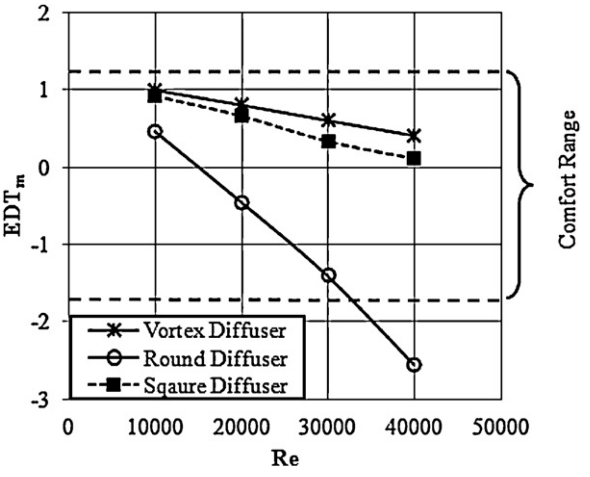

Fig. 12. Mean effective draft temperature in room at different Reynolds numbers.

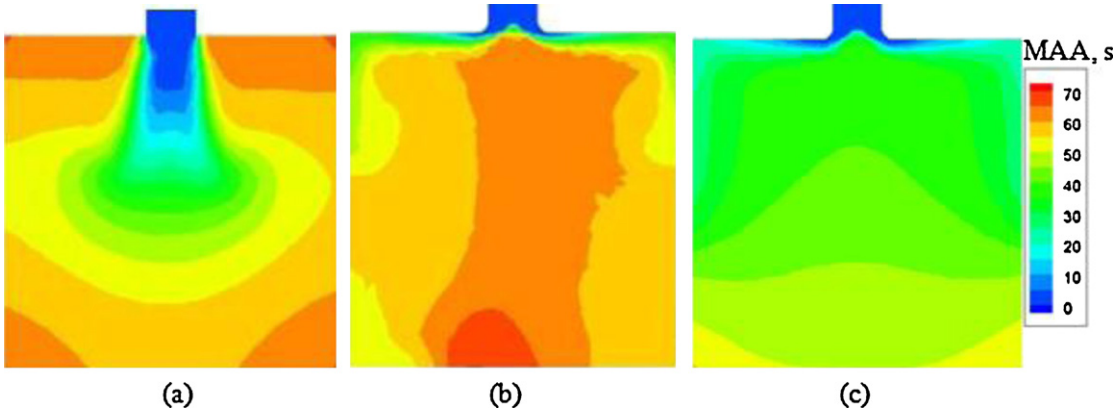

Fig. 13. Mean age of the air distribution for (a) vortex, (b) round, and (c) square diffuser.

in the room increases by about 2%. This can be explained referring to Fig. 9 where the vortex diffuser demonstrates the highest value of the dimensionless mean relative humidity because it has the lowest room temperature while the value of the square and the round diffuser is nearly same.

Fig. 12 shows the mean effective draft temperature within the room at different inlet velocities for the three studied diffusers. From this figure, it can be seen that, as the inlet velocity increases, the mean value of the effective draft temperature decreases and vice verse. The vortex diffuser demonstrates the highest values where the round diffuser demonstrates the lowest one. The comfort conditions achieved by the round diffuser diminish when Reynolds number is over 30,000.

Fig. 13 shows the distribution of the mean age of the air in the room for the three considered diffusers. From this figure, it can be seen that the value of the mean age of the air in case of the vortex and round diffuser is nearly the same and larger than the square diffuser. The stratification of the MAA is well established in case of the square diffuser. This can be attributed to the buoyancy force raises the flow upward and it has a great effect on the path lines of the air inside the room.

The lower values of the mean age of the air do not allow the air to exchange the heat with the walls. This means that the air is extracted from the room with low temperature. Hence, the ventilation effectiveness is small for the square diffuser and high for the round one as shown in Fig. 14.

5.3. Diffuser velocity decay coefficient

The performance of the jet created by the diffuser can be characterized by a single constant, namely jet velocity decay coefficient (K). It can be defined as [19]:

$$\frac{V}{V_o} = K\frac{\sqrt{A_o}}{x} \tag{18}$$

The diffuser velocity decay coefficient (K) can be determined by plotted the dimensionless velocity (V/V_o) versus the dimensionless distance ($x/\sqrt{A_o}$) as shown in Fig. 15 where the values of the decay coefficient can be directly determined when the curve intersects the dimensionless velocity at the unity (i.e. $V/V_o = 1$). The values of the velocity decay coefficient are tabulated in Table 3.

5.4. Effect of swirling angle of the vortex diffuser

The swirling angle is the inclination of the diffuser blades on the vertical plane. The effect of three values of swirling angle namely 30°, 45°, and 60° is investigated where inlet velocity is 1 m/s, inlet

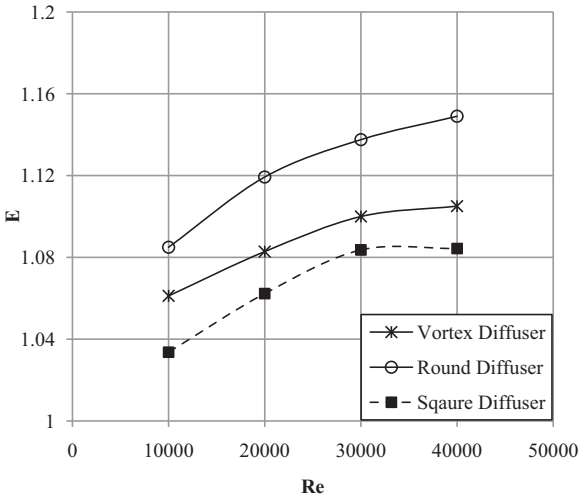

Fig. 14. Ventilation effectiveness at different Reynolds number at same inlet temperature and relative humidity for tested diffusers.

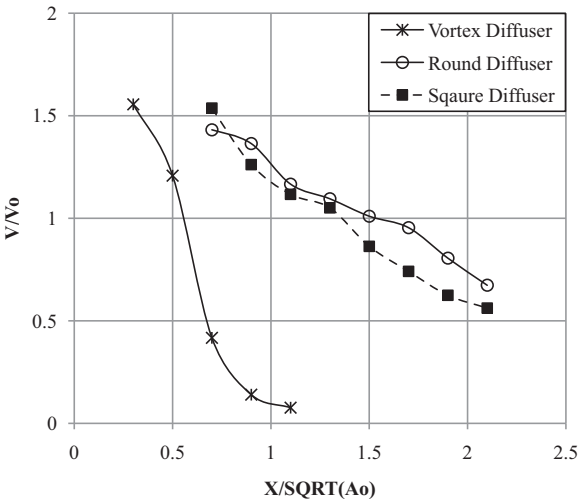

Fig. 15. Dimensionless velocity for the vortex, square, and round diffusers.

Table 3
Velocity decay coefficient for the three tested ceiling diffusers.

Diffuser type	Velocity decay coefficient
Vortex	0.57
Square	1.4
Round	1.5

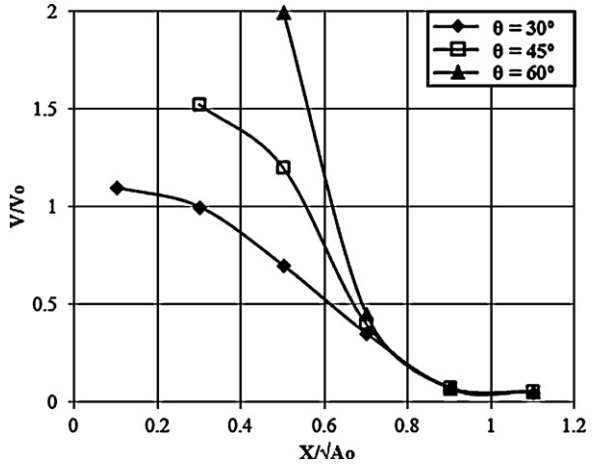

Fig. 16. Dimensionless velocity for different swirling angles for vortex diffuser.

Table 4
Velocity decay coefficient for vortex diffuser.

Swirling angle	K	C_p
30°	0.3	0.88
45°	0.57	2.20
60°	0.61	7.65

temperature is 18 °C, isothermal walls at 28.5 °C, and isothermal ceiling at 27 °C.

Fig. 16 shows that the inclination angle of 60° has the longest throw but it has the highest pressure coefficient (C_p) as tabulated in Table 4.

6. Conclusions

A set of the experimental and numerical investigation to study the performance of the vortex, round, and square ceiling diffusers has been reported for various inlet velocities. CFD, an important tool in HVAC engineering, is used to analyze the data generated by models representing the complexity of the flow patterns that evolve inside the ventilated spaces. The standard k–ε turbulence model can be used to simulate the vortex, square, and round ceiling diffusers. This result is also considered in other papers [20].

The velocity vector of the vortex ceiling diffuser exhibits three specified regions namely: main swirling stream regions of the primary flow, upper recirculation region at the end of the jet, and lower region without any recirculation or swirling flow. The buoyancy force has a great effect on temperature and velocity field, and the thermal comfort zone created by the three diffusers is large and wide but diminished in case of the round diffuser when the Reynolds number increases over 30,000.

The vortex diffuser makes the room colder than the square and round diffuser. It consumes energy about 1.5 times less than square diffusers hence, it saves energy of the supply fan.

The velocity decay coefficient of square and round diffuser is nearly same and is 2.6 times more than the velocity decay coefficient of the vortex diffuser with 45° swirling angle accordingly; the vortex diffusers with 45° swirling angle are suitable and preferable for the high-rises buildings because it has suitable throw and its jet is focused on the room center also, it saves the consumption energy.

References

[1] A.F. Alfahaid, Effects of Ventilation on Human Thermal Comfort in Rooms 45, Ph.D. Thesis, Old Dominion University, Norfolk, VA, 2000.
[2] A.H. Al-Hamed, Determining Velocity, Temperature and Occupancy Comfort within a 3-D. ROOM, M.Sc. Thesis, King Fahd University, Saudi Arabia, 1990.
[3] H.B. Awbi, Ventilation of Buildings, second ed., Spon Press, 2003.
[4] ASHRAE Handbook, Fundamentals, 2008.
[5] ASHRAE Standards, Standard 55, 1992.
[6] J. Abanto, D. Barrero, M. Reggioa, B. Ozell, Airflow modeling in a computer room, Building and Environment 39 (2004) 1393–1402.
[7] M. Bartak, M. Cermak, J.A. Clarke, J. Denev, F. Drkal, M. Lain, I.A. Macdonald, M. Majer, P. Stankov, Experimental and numerical study of local mean age of air, in: Seventh International IBPSA Conference, Rio de Janeiro, Brazil, August 13–15, 2001.
[8] G. Gan, Evaluation of room air distribution systems using computational fluid dynamics, Energy and Buildings 23 (1995) 83–93.
[9] J.D. Spitler, An Experimental Investigation of Air Flow and Convective Heat Transfer in Enclosures Having Large Ventilative Flow Rates, Ph.D. Thesis, University of Illinois at Urbana-Champaign, 1990.
[10] P.V. Nielsen, Velocity distribution in a room ventilated by displacement ventilation and wall-mounted air terminal devices, Energy and Buildings 31 (3) (2000) 179–187.
[11] J. Srebric, Q. Chen, Simplified numerical models for complex air supply diffusers, HVAC&R Research 8 (3) (2002) 277–294.
[12] L. Zhou, F. Haghighat, Simplified Method for Modeling Swirl Diffusers, Department of Building, Civil and Environmental Engineering Concordia University, Montreal, Canada, 2007.
[13] G. Einberga, K. Hagstrom, CFD modeling of an industrial air diffuser predicting velocity and temperature in the near zone, Building and Environment 40 (2005) 601–615.
[14] FLUENT Inc., User's Guide for FLUENT/UNS, Release 6.3, Lebanon, USA, 2006.
[15] S.C. Hu, Airflow characteristics in the outlet region of a vortex room air diffuser, Building and Environment 38 (2003) 553–561.
[16] J.L. Lumley, H. Tennekes, A First Course in Turbulence, MIT Press, London, England, 1972.
[17] T.B. Gatski, M.Y. Hussaini, J.L. Lumley, Simulation and Modeling of Turbulent Flows, Oxford University Press, New York, Oxford, 1996.
[18] J.H. Ferziger, M. Peric, Computational Methods for Fluid Dynamics, Springer Verlag, Berlin, Germany, 1996.
[19] S. Shakerin, P.L. Miller, Experimental Study of Vortex Diffusers, University of the Pacifica, November 1995.
[20] F. Kuznik, G. Rusaouen, J. Brau, Experimental and numerical study of a full scale ventilated enclosure: comparison of four two equations closure turbulence models, Building and Environment 42 (2007) 1043–1053.